Asymmetrical Voltage Cancellation Control for ZVS Series Resonant Inverter for Induction Heating System using IP Structure

M. HELAIMI, D. BENYOUCEF, B. BELMADANI and R. TALEB
Laboratory of Electrical Engineering and Renewable Energies
Department of Electrical Engineering
University of Chlef
BP151, Hay Essalam, Chlef
halimi1976@yahoo.fr

Abstract **- This paper presents two efficient techniques for output power control of a series resonant inverter induction heating system using PI control and IP control. One of the most important problems associated with the proposed inverter is achieving ZVS operating during the heating cycle. To overcome this problem, asymmetrical voltage cancellation (AVC) control technique is proposed. The phased look loop (PLL) is used to track the switching frequency. The complete closed loop control model is obtained using a small signal analysis. The validity of the proposed control is verified by simulation results. They show the superiority of IP controller over PI controller.**

Index Terms – Induction Heating, PI-Controller, IP-Controller, PLL, ZVS Operation, AVC Control

I. INTRODUCTION

Nowdays, Induction heating is the most controllable method for applying heat in a number for industrial applications including surface hardening, melting and brazing. It's based on the following two laws: Electromagnetic induction and the Joule effect [1].

In recent application, two resonant inverter topologies (series or parallel) are used in induction heating system to achieve ZVS or ZCS by employing the resonant circuit [2]. Depending on a high power density and improved reliability, the full-bridge series resonant inverter based on IGBT's or MOSFET's is the most used topology [3].

In order to improve the conversion efficiency, different control strategies have been proposed including: Asymmetrical duty-cycle (ADC) control [4-5], phase-shift (PS) control [6] and asymmetrical voltage-cancellation (AVC) control [3], [7]. The AVC control allows all the switches to be turned-on with zero voltage with the minimum switching frequency [3].

Most applications involve heating the work-piece at a given temperature for a given time. During the heating cycle, the electrical resistivity $\boldsymbol{\rho}$ and relative magnetic permeability $\boldsymbol{\mu_r}$ vary, especially when the work-piece reaches the Curie temperature [3]. Load power regulation is important for high quality heating system. Generally, the traditional PI controller is widely used to regulate the output power of the resonant inverter.

In this paper, a series resonant inverter with AVC control technique is proposed. The proposed control scheme is based on two control loops: frequency control loop and power control loop. The first is used to track the resonant frequency to achieve ZVS operation during the heating cycle and the second is used to adjust the switch duty cycle in the event of load parameter variation.

To improve good transit performances by attenuation of the overshoot and a rise time, an IP controller is employed. The small signal model is used to analyze the performance of a control loops.

This paper is organized as follow: Detailed circuit diagram and the proposed control scheme are given in Section 2 and 3. Open loop small signal analysis is presented in Section 4. The final closed loop control with both PI and IP structure is introduced in Section 5. Some simulation results are presented and discussed in Section 6. Finally Section 7 concludes this paper.

II. CIRCUIT DESCRIPTION

A number of induction-heating resonant inverters have been reported in literature. However, they all employ the basic conversion process of AC-DC rectification of the phase source and followed by a single phase higher frequency stage [3], [6]. Figure 1 show the proposed configuration used in this work:

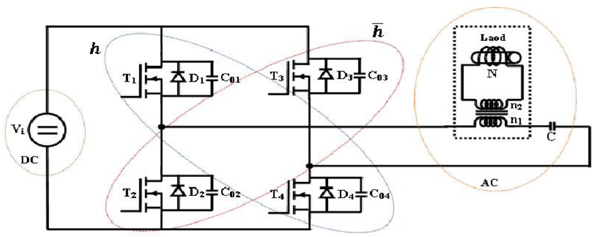

Fig. 01: Full bridge series resonant inverter

It consists of four IGBT transistors with anti-parallel diodes and the resonant tank. The induction heating load constitutes a **50 CrV4** carbon steel billet placed inside N-turns cooper coil at specific air gap. The induction heating load can be modelled by means of a series combination of its equivalent resistance $\boldsymbol{R}$ and equivalent inductance $\boldsymbol{L}$ [8].

III. PROPOSED CONTROL STRATEGY

The AVC control technique shown in Figure 2 is based on the comparison of the reference power signal $\boldsymbol{P_{ref}}$ to the actual power signal $\boldsymbol{P}$. The delivered power is controlled by adjusting the switch duty cycle $\boldsymbol{D}$ in the event of load parameter changes. The frequency control loop (PLL) is used to track the resonant frequency in order to maintain ZVS during the heating process. It's composed of: a zero crossing detector, a phase detector, a low-pass filter and a VCO [7].

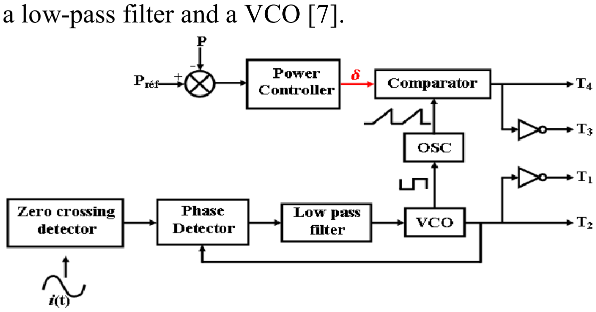

Fig. 02: Bloc diagram of the proposed control system

The AVC control signal is created by comparing the signal $\boldsymbol{\delta}$ with a ramp signal as shown in Figure 3 [7]:

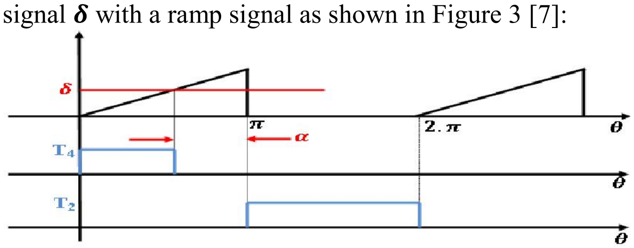

Fig. 03: Waveforms of the asymmetrical gate drive signal

The $\mathbf{T_1}$ and $\mathbf{T_3}$ signals are inversed of $\mathbf{T_2}$ and $\mathbf{T_4}$ signals, respectively.

IV. OPEN LOOP SYSTEM

The diagram in figure 4 shows the open loop system in the form of a block diagram. Each element of the control system is represented by a block and these are joined by lines with arrows showing the sequence of controls [4-5].

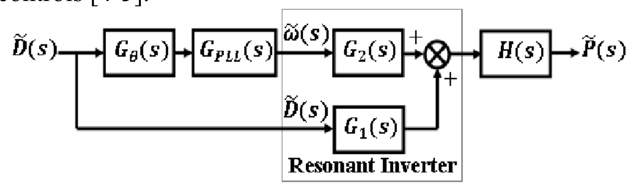

Fig. 04: Open loop small signal model

The transfer function from the duty cycle $\widetilde{\boldsymbol{D}}$ to the output power $\widetilde{\boldsymbol{P}}$ is giving by:

$$G(s) = [G_\theta(s).G_{PLL}(s).G_2(s) + G_1(s)].H(s) \qquad (1)$$

The transfer function of a phase detector is:

$$G_\theta(s) = \pi \qquad (2)$$

The closed-loop transfer function for a second order PLL can be written as:

$$G_{PLL}(s) = \frac{2.\xi.\omega_n.s^2 + \omega_n^2.s}{s^2 + 2.\xi.\omega_n.s + \omega_n^2} \qquad (3)$$

where $\boldsymbol{\omega_n}$ is the natural frequency and $\boldsymbol{\xi}$ is the damping factor.

There have been several approaches reported in literature to get small signal modeling. In this paper, the small signal circuit of the series resonant inverter with the proposed control is obtained using the extending description function (EDF) technique [6], [9]. The small signal transfer function $\boldsymbol{G_1(s)}$ and $\boldsymbol{G_2(s)}$ are expressed as follows:

$$G_1(s) = C_s.(s.I - A_s)^{-1}.B_{1s} \qquad (4)$$

$$G_2(s) = C_s.(s.I - A_s)^{-1}.B_{2s} \qquad (5)$$

where:

$$A_s = \begin{bmatrix} \frac{-R}{L} & -\omega_e & \frac{-1}{L} & 0 \\ \omega_e & \frac{-R}{L} & 0 & \frac{-1}{L} \\ \frac{1}{C} & 0 & 0 & -\omega_e \\ 0 & \frac{1}{C} & \omega_e & 0 \end{bmatrix}$$

$$B_{1s} = \begin{bmatrix} \left(\frac{Vi}{L}\right).cos(pi.D_e) \\ -\left(\frac{Vi}{L}\right).sin(pi.D_e) \\ 0 \\ 0 \end{bmatrix}$$

$$B_{2s} = \begin{bmatrix} -I_{qe} \\ I_{de} \\ -V_{cqe} \\ V_{cde} \end{bmatrix}$$

$$C_s = R.[I_{de} \quad I_{qe} \quad 0 \quad 0]$$

A first order low-pass filter can be described in Laplace notation as:

$$H(s) = \frac{1}{\tau.s + 1} \tag{6}$$

The operating point is given in the **Appendix A**.
The Bode plot of the open loop transfer function $\boldsymbol{G(s)}$ is shown in Figure 5:

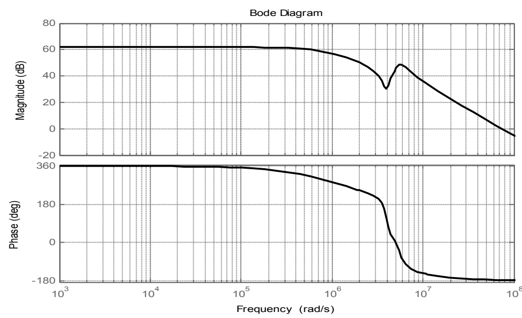

Fig. 05: Bode plot of the open loop system

Figure 5 shows the resulting Bode stability margins:

$G_m = -34.8$
$P_m = 4.32°$

The pole of $\boldsymbol{G(s)}$ are found to be:

$p_{1,2} = (-0.7386 \pm 5.4879.i).10^6$
$p_{3,4} = (-0.0032 \pm 0.0032.i).10^6$
$p_{5,6} = (-0.7385 \pm 0.1557.i).10^6$
$p_7 = -2.8218.10^6$

Thus this system is stable since the real parts of the poles are negative.

V. Closed Loop Control

The control objectives are to regulate the output power to its reference as fast and with as little overshoot as possible, despite changes in the input voltage $\boldsymbol{V_i}$ or changes in the load, to achieve and maintain ZVS operation during the heating process. To express these control objectives two closed loop control system are proposed:

A. PI control system

A PI controller is a generic control loop feedback mechanism widely used in industrial heating systems. Its attempts to minimize the error by adjusting the process control inputs. Figure 6 shows the block diagram of the linearized control system, including a linear plant $\boldsymbol{G(s)}$ and a classic PI controller.

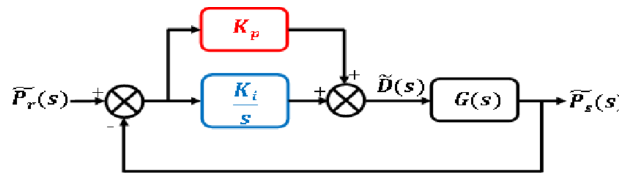

Fig. 06: Closed loop control system with PI structure

$\boldsymbol{G(s)}$ is the transfer function of the linear plant, expressed in (1). A PI controller has the transfer function:

$$C(s) = K_p.\left(1 + \frac{K_i}{s}\right) \tag{7}$$

where $\boldsymbol{K_p}$ is the proportional gain and $\boldsymbol{K_i}$ is the integral. The closed loop transfer function between the output $\boldsymbol{\tilde{P}_s(s)}$ and the input $\boldsymbol{\tilde{P}_r(s)}$ is given by:

$$\frac{\tilde{P}_s(s)}{\tilde{P}_r(s)} = \frac{(K_p.K_i + K_p.s).G(s)}{s + (K_i + s).K_p.G(s)} \tag{8}$$

The $\boldsymbol{K_p}$ and $\boldsymbol{K_i}$ values of PI controller are determined by Ziegler-Nichols methods.

B. IP control system

In process industries, the main objective of the I-P controller is to make the peak overshoot, settling time and final steady state error, as small as possible. The closed loop control system as shown in Figure 7 [10-11]:

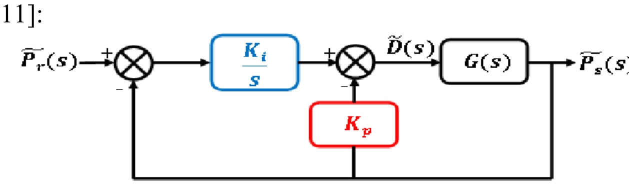

Fig. 07: Closed loop control system with IP structure

The output signal from the I-P controller is:

$$\tilde{D}(t) = K_i.\int_0^t e(t).dt - K_p.\tilde{P}_s(t) \tag{9}$$

The closed loop transfer function between the output $\boldsymbol{\tilde{P}_s(s)}$ and the input $\boldsymbol{\tilde{P}_r(s)}$ is given by:

$$\frac{\tilde{P}_s(s)}{\tilde{P}_r(s)} = \frac{K_i.G(s)}{s + (K_i + K_p.s).G(s)} \tag{10}$$

The $\boldsymbol{K_p}$ and $\boldsymbol{K_i}$ values of I-P controller are determined by Hall-Sartorius methods [12].

VI. Simulation and Comparison

In this section, we evaluate, through computer simulation, the ability of the proposed controller to regulate the output power of the system modeled in

Section 4. Figure 8 shows the closed loop response with both the conventional PI and the IP controllers:

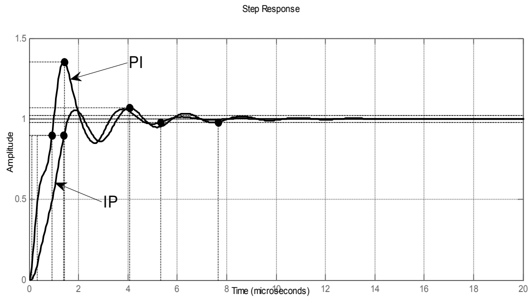

Fig. 08: Closed loop response of the system

Some performance characteristics for the feedback control systems with the two proposed controllers are summarized in Table I:

TABLE I: SOME PERFORMANCE CHARACTERISTICS

Controller	PI	IP
K_p	0.0073	0.0076
K_i	$6.69.10^5$	$5.55.10^3$
G_m	9.02	29.5
P_m	$47.5°$	$136.7°$
Overshoot	35.33%	6.75%
t_r	$0.8\mu s$	$1.08\mu s$
ISE	$3.57.10^{-7}$	$6.9.10^{-7}$

Robustness is an important consideration in control design. The tradeoff between the robustness and performance must be taken into account when comparing the performance of different control structures.

To study the system robustness we introduce a variation of $\pm 20\%$ of R and $\pm 10\%$ of V_i in the nominal plant. The results obtained are presented in Figure 9 (a-d), respectively.

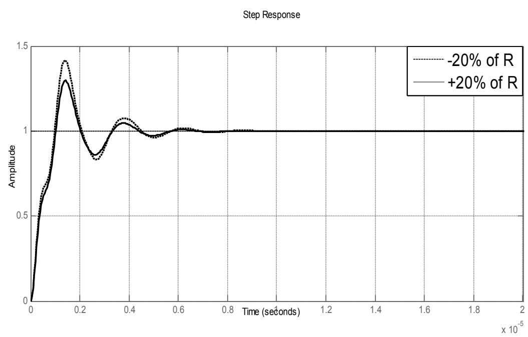

(a) PI controller

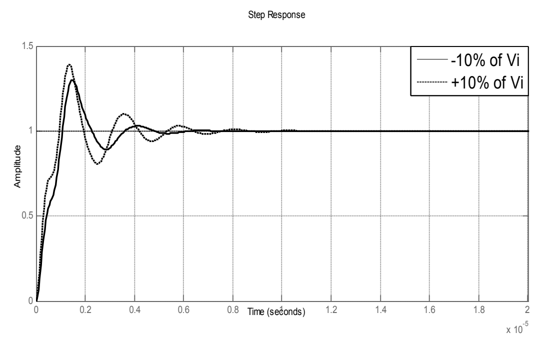

(b) PI controller

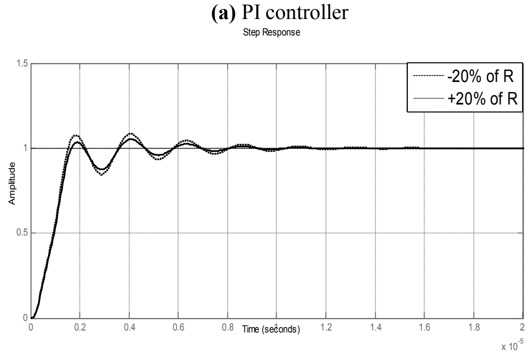

(c) IP controller

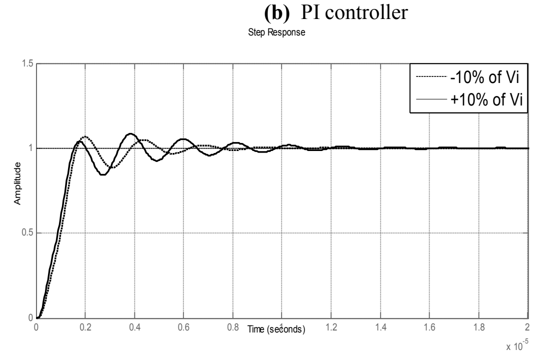

(d) IP controller

Fig. 9: Robustness to load and line variation

It is important to note that the IP control system gives the better overall response compared to the PI controller.

VII. CONCLUSION

In this paper, analysis, simulation and implementation of IP controller for series resonant inverter induction heating system are presented. The output power of the proposed inverter is adjusted by acting on duty cycle and switching frequency. The main advantages of the IP control scheme are fast response, soft switching and resonant tracking with a good heating performance. The proposed IP controller can be effectively implemented for other inverter topologies or complex structured nonlinear systems controlled using DSP processor or FPGA.

APPENDIX

The operating point is given in the Table II:

TABLE II: OERATING POINT

R	$10\ \Omega$
L	$6.77\ \mu H$
C	$19.3\ n.F$
V_i	$136\ v$
D_e	$25\ \%$
ω_e	$2.82.10^6\ rad/s$
I_{de}	$3.776\ A$
I_{qe}	$-9.5468\ A$
V_{cde}	$177.1146\ v$
V_{cqe}	$69.3456\ v$

REFERENCES

[1] A. NAMADMALAN and J. S. MOGHANI, “Single-Phase Current Source Induction Heater with Improved Efficiency and Package Size”, Journal of Power Electronics, Vol. 13, No. 2, pp. 322-328, March 2013.

[2] G. BAL, S. ONCU and E. OZBAS, “Self-Oscillated Induction Heater for absorption Cooler”, ELEKTRONIKA IR ELEKTROTECHNIKA, Vol. 19, N° 10, pp. 45-48, 2013.

[3] J. M. BURDIO, L. A. BARRAGAN, F. MONTERDE, D. NAVARRO and J. ACERO, «Asymmetrical voltage-cancellation control for full-bridge series resonant inverters», IEEE Transactions on Power Electronics, Vol.19, N°02, pp. 461-469, 2004.

[4] J. TIAN, J. PETZOLDT, T. REIMANN, M. SCHERF, G. BERGER, "Modeling of Asymmetrical Pulse Width Modulation with Frequency Tracking Control using Phasor Transformation for Half-Bridge Series Resonant Induction Cookers", 11th European Conference on Power Electronics and Applications (EPE), September, 2005, Dresden, Germany.

[5] J. TIAN, J. PETZOLDT and T. RIEMANN, M. SCHERF and G. BERGER, “Control system analysis and design of a resonant inverter with the varaiable frequency variable duty cycle”, European Conference on Power Electronics and Applications (EPE), 2005, Dresden, Germany.

[6] L. GRAJALES and F.C. LEE “Control system design and small signal analysis of a phase shift controlled series resonant inverter for induction heating”, in PESC Record- IEEE Power Electronics Specialists Conference, 1995, pp 450-456.

[7] S. CHUDJUARJEEN, A. SANGSWANG, and C. KOOMPAI, "An Improved LLC Resonant Inverter for Induction-Heating Applications with Asymmetrical Control", IEEE Transactions on Industrial Electronics, vol. 58, N°7, pp. 2915-2925, Jully 2011.

[8] N. A. AHMED, “Three-phase High frequency AC conversion circuit with dual mode PWM/PDM control strategy for high power IH applications”, PWASET Vol.35, pp 371-377, Novembre 2008.

[9] E. X. YANG, F. C. LEE and M. M. JOVANOVIC, “Small signal modeling of power electronic circuits using extended describing function technique”, in Proc. VPEC, 1991, pp 167-178.

[10] M. A. ZANJANI, G. H. SHAHGHOLIAN, S. ESHTEHARDIHA, “Gain Tuning PID and IP Controller with an Adaptive Controller Based on the Genetic Algorithm for Improvement Operation of STATCOM”, 7th WSEAS International Conference on Electric Power Systems, High Voltages, Electric Machines, Venice, Italy, November 21-23, 2007.

[11] S. SINGH, S. GUPTA and N. TIWARI, “FPGA Implementation of Discrete IP+PWM Controller for Double Boost DC to DC Converter”, International Journal of Advanced Research in Computer Science and Software Engineering, Vol. 03, N° 09, pp. 1007-1013 September 2013.

[12] K. BETTOU, A. CHAREF “Control Quality Enhancement Using Fractional $PI^{\lambda}D^{\mu}$ Controller”, Int. Journal of Sciences an d Systems, Vol. 40, N°08, pp. 875-888, August. 2009.